

Prevention of resistive wall tearing mode major disruptions with feedback

H. R. Strauss^{1, 1}

¹ HRS Fusion, West Orange, NJ 07052

Abstract

Resistive wall tearing modes (RWTM) can cause major disruptions. A signature of RWTMs is that the rational surface is sufficiently close to the wall. For $(m, n) = (2, 1)$ modes, at normalized minor radius $\rho = 0.75$, the value of q is $q_{75} < 2$. This is confirmed in simulations and theory and in a DIII-D locked mode disruption database. The $q_{75} < 2$ criterion is valid at high β as well as at low β . A very important feature of RWTMs is that they produce major disruptions only when the $q_{75} < 2$ criterion is satisfied. If it is not satisfied, or if the wall is ideally conducting, then the mode does not produce a major disruption, although it can produce a minor disruption. Feedback, or rotation of the mode at the wall by complex feedback, can emulate an ideal wall, preventing major disruptions. The q_{75} criterion is analyzed in linear simulations, and a simple geometric model is given.

1 Introduction

Resistive wall tearing modes (RWTM) can cause cause major disruptions. This is based on evidence from theory, simulations, and experimental data [1, 2, 3, 4, 5, 6]. For example, DIII-D locked mode shot 154576 [7] experienced a major disruption. Linear simulations [3] found the reconstructed equilibrium was stable with an ideal wall. and found a scaling of the linear growth rate with the wall penetration time. Nonlinear simulations found a complete thermal quench, and agreement with the experimental thermal quench (TQ) time and the amplitude of the perturbed magnetic field.

A signature of RWTMs is that the rational surface is sufficiently close to the wall. For $(m, n) = (2, 1)$ modes, the rational surface radius of the $q = 2$ surface, normalized to the plasma minor radius, is $\rho_{q2} > 0.75$. This can also be expressed as the value of q at $\rho = 0.75$, $q_{75} < 2$. This is confirmed in simulations and theory. Experimentally, it is the disruption criterion in a DIII-D locked mode disruption database. The importance of mode locking and disruption precursors is discussed. The $q_{75} < 2$ criterion is valid at high β as well as at low β . This is verified experimentally as well as in simulations.

A very important feature of RWTMs is that they produce major disruptions when the $q_{75} < 2$ or $\rho_{q2} > 0.75$ criterion is satisfied. If the wall is ideally conducting, then

¹Author to whom correspondence should be addressed: hank@hrsfusion.com

the mode becomes a tearing mode and does not produce a major disruption, although it can produce a minor disruption. Feedback, or rotation of the mode at the wall by complex feedback, can emulate an ideal wall. This implies that RWTMs can be made to act like tearing modes with an ideal wall, and only produce minor disruptions. This is verified experimentally and in simulations at low and high β .

The q_{75} criterion for a RWTM implies that the $q = 2$ rational surface is sufficiently close to the wall to interact with it. This is analyzed in a linear model, and a simple geometric model is given of the wall interaction criterion. The criterion depends weakly on the ratio of ρ_{q2}/ρ_w , where ρ_w is the wall radius normalized to plasma radius. For $\rho_w > 1.5$, the wall is too far away for a RWTM and feedback stabilization is not possible. The criterion is also obtained for general (m, n) , and requires the rational surface to be closer to the wall.

The outline of the paper is as follows. The domain of instability of RWTMs in the (q_{75}, β) plane is presented qualitatively in Sec.2. Also shown is the $\rho_{q2} > 0.75$ database of DIII-D locked mode disruptions. The relevance of mode locking, precursors, edge cooling, and current contraction are discussed. In Sec.3, simulations are presented of a sequence of equilibria in which major disruptions occur with a resistive wall, when $q_{75} < 2$, otherwise a minor disruption occurs. If the wall is ideal, only a minor disruption occurs. In a particular example, it is demonstrated that feedback or wall rotation give a similar result as an ideal wall. The amplitude of the non axisymmetric $n > 1$ perturbations is much larger when the wall is resistive, in comparison with an ideal wall, feedback or rotating wall. The computational model used for feedback and rotating wall is discussed in Sec.4. Finite β experimental results in NSXT are presented in Sec.5. The experiment shows a feedback limited tearing mode, with $\rho_{q2} \approx 0.75$, evidently close enough to the wall to be feedback controlled. Sec.6 shows simulations based on an NSTX intermediate β_N equilibrium. For a resistive wall, a major disruption occurs. With an ideal wall, feedback, or rotating wall, only minor disruptions occur. The amplitude of the $n > 1$ perturbations is much larger for a resistive wall than for ideal wall, feedback, or rotating wall, as in Sec.3. The reason for the q_{75} criterion is analyzed in Sec.7. The critical value of ρ_{q2}/ρ_w is obtained from linear stability of model equilibria. It is in good agreement with a simple geometric model. The $\rho_{q2} > 0.75$ criterion occurs for $\rho_w = 1.2$, as in DIII-D, the model equilibria of Sec.3, and NSTX. The critical ρ_{q2} depends weakly on ρ_w , for $\rho_w \leq 1.5$. A summary is provided in Sec.8.

2 RWTM parameter space

The expression $\rho_{q2} = 0.75$, can be written as $q_{75} = 2$, where $q_{75} = q(\rho_{q2} = .75)$, which is useful to represent the RWTM unstable parameter space. Fig.1(a) gives a schematic

parameter space (q_{75}, β) of RWM and RWTMs. The RWTM is unstable for $q_{75} \leq 2$. The RWM beta limit is approximately the Troyon [9] no wall limit β_N . The RWTM is unstable below the RWM limit [10, 11]. The labeled points correspond to low and high β examples in Sec.3, Sec.5, and Sec.6. Both low and high β RWTM and RWM can be limited to minor disruptions by feedback, rotation, or an ideal wall. Locking with resistive wall and without feedback or rotation allows a major disruption.

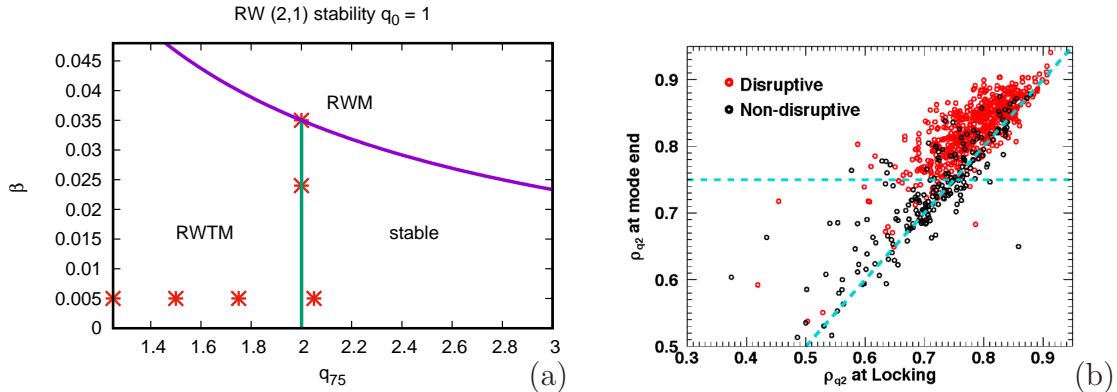


Figure 1: (a) Schematic diagram of RWM and RWTM stability in (q_{75}, β) space. (b) Disruptivity in a DIII-D locked mode disruption database. Reproduced from [8]

Fig.1(b) shows a database of DIII-D disruptivity [8] which depends on ρ_{q2} . The onset is $\rho_{q2} = .75$ or $q_{75} = 2$. Nearly all disruptions occur for $\rho_{q2} > 0.75$. The disruptions occur for locked modes. Mode locking means that toroidal rotation stops, destabilizing tearing modes [7, 12]. Sheared rotation stabilizes tearing modes [14, 13, 15], including RWTMs [16].

Fig.1(b) also shows that ρ_{q2} tends to increase between mode locking and the disruption. This could be explained by edge cooling, which produces current contraction [17, 18], and can cause ρ_{q2} to increase. A current contraction model [5] is discussed in Sec.7. Current contraction is caused by edge cooling, which in turn can have several causes. One possible cause is overlapping tearing modes in the edge region, called a $T_{e,q2}$ collapse [7]. Another possibility is resistive ballooning turbulence, proposed as an explanation of the Greenwald density limit [19]. Another possible cause of edge cooling is impurity radiation [20]. The impurity content might be raised by increasing the plasma density to the Greenwald limit [21]. The impurities might be introduced purposefully, as in massive gas injection [22], or accidentally, as UFOs, pieces of plasma facing tiles falling into the plasma. All these have been called causes of disruptions, but they are really precursors, cooling the edge and destabilizing a RWTM.

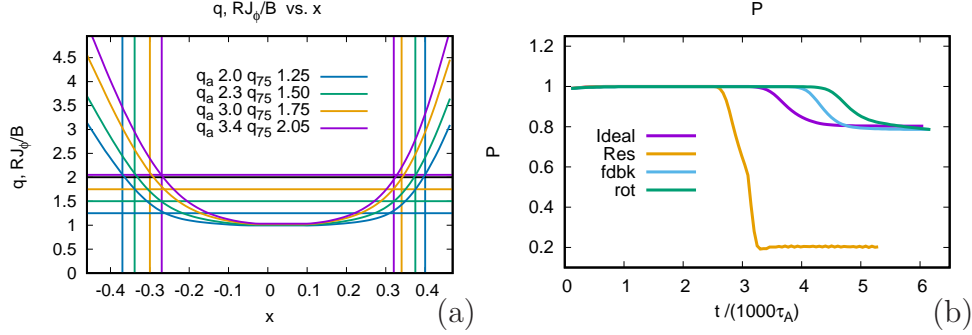


Figure 2: (a) q profiles of model equilibria as a function of major radius $x = R - R_0$ for model equilibria with $q_a = 2, 2.3, 3, 3.4$. All but $q_a = 3.4$ have $q_{75} < 2$. (b) time histories of case $q_a = 3$ with ideal, resistive, feedback, and rotating wall boundary conditions. In all but the resistive wall case, only a minor disruption occurs.

3 Low β RWTM disruptions

Simulations were performed with M3D [24] for a sequence of modified MST equilibria [5, 6]. Here the results are extended by including simulations with feedback and wall rotation, as discussed in Sec.4. The simulations had parameters: Lundquist number $S = 10^5$, wall Lundquist number $S_w = \tau_w/\tau_A = 10^3$, where τ_w is the wall penetration time and τ_A is the Alfvén time, and parallel thermal conductivity $\kappa_{\parallel} = 10R^2/\tau_A$. The simulation had 16 toroidal planes. Fig.2 shows $q(x)$ profiles for a sequence of modified MST equilibria [5] with $\rho_w = 1.2$. The profiles have $q_0 = 1$ and edge $q_a = 2, 2.3, 3, 3.4$. For $q_a \leq 3$, $q_{75} < 2$, so the equilibria are unstable to RWTM. The case $q_a = 3.4$ is RWTM marginally stable. Nonlinear simulations with M3D [24] were initialized with these equilibria. It was shown [5] that with an ideal wall, all the equilibria are unstable only to minor disruptions. For $q_a \leq 3$, $q_{75} < 2$, with a resistive wall, major disruptions occur. If $q_{75} > 2$, and the wall is resistive, the disruption is minor. The particular case $q_a = 3$, $q_{75} = 1.75$ is considered in more detail. Fig.2 (b) shows time histories of total pressure P for the case $q_a = 3$, with ideal wall, resistive wall, feedback, and wall rotation. A major disruption occurs for a resistive wall. All the other boundary conditions give only minor disruptions. Fig.3 shows contours of pressure and perturbed magnetic field in nonlinear simulations corresponding to the time histories in Fig.2, including feedback and wall rotation. The simulations demonstrate that ideal wall, feedback, and rotating wall limit growth of tearing mode. A resistive wall (or no wall) allows a tearing mode to reach much larger amplitude than an ideal wall, or similar boundary conditions. Contours of pressure p are shown near the last times in the history plot Fig.2. The contour plots correspond to boundary conditions (a) ideal wall, (b) resistive wall with no rotation, (d) feedback, and (e) edge rotation. Boundary conditions (d) and (e) are similar to (a), with small perturbations and only minor

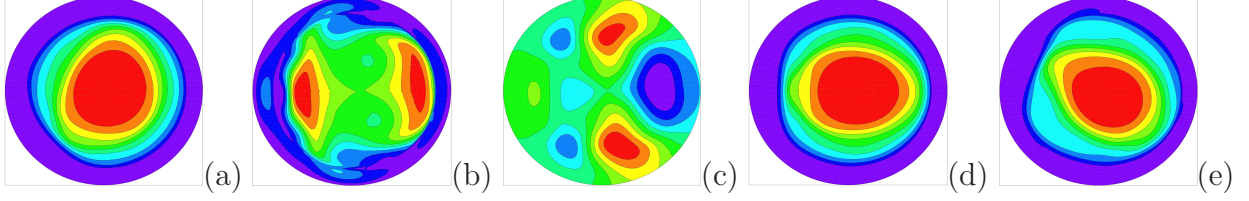


Figure 3: *Pressure p contours in nonlinear simulation of the q_a case for (a) ideal wall, (b) resistive wall, (c) perturbed $n \geq 1$ part of magnetic field corresponding to case (b), (d) feedback stabilization, (e) rotating wall. Fig.3(a),(b) reproduced from [6]*

disruptions. In (c), perturbed magnetic flux ψ contours correspond to the pressure contours in (b). The perturbed flux is relevant to the analysis of ρ_{q2} in Sec.7. The feedback and wall rotation is described in [6] and summarized in the following Sec.4.

4 Feedback

Active feedback and wall rotation can make the wall effectively ideal and suppress RWTM major disruptions. There have been extensive theoretical [25, 26, 27] and experimental studies of feedback stabilization [28, 29, 30]. To model feedback, consider the magnetic diffusion equation at a thin resistive wall [1, 3, 16]

$$\frac{\partial \psi_w}{\partial t} = \frac{\eta_w}{\delta_w} (\psi'_{vac} - \psi'_p) - \Omega_w \frac{\partial \psi}{\partial \phi}. \quad (1)$$

where ψ_w is the magnetic potential at the wall, ψ'_p is its radial derivative on the plasma side of the wall, η_w, δ_w are the wall resistivity and thickness, and ψ'_{vac} is the radial derivative of ψ_w on the vacuum side of the wall. The vacuum field is taken of the form

$$\psi_{vac} = \psi_w \left(\frac{r_w}{r} \right)^m + \psi_f \left[\left(\frac{r_w}{r} \right)^m - \left(\frac{r}{r_w} \right)^m \right] \quad (2)$$

where $\psi_f = gD\psi_w/2 - hr_w F\psi'_p/(2m)$ is the feedback signal, g is the normal gain, h is the transverse gain, $D(\theta, \psi_w), F(\theta, \psi_w)$ are screening functions of poloidal and toroidal angle of the wall, modeling the location of the sensors, and r_w is the wall radius. For now, take $D = F = 1$. They could be taken non zero in future numerical studies, and might affect detailed predictions of the modeling. The g term models saddle coils which sense $b_n \propto \psi_w$, while h models probes which sense transverse perturbed magnetic field $b_l \propto \psi'_p$. The Ω_w term models a rotating wall boundary condition [23, 27]. Wall rotation can provide electromagnetic torque to sustain sheared rotation [23].

Then (1),(2) can be expressed

$$\frac{\partial \psi_w}{\partial t} = -\frac{m}{\tau_{wall}} [(1-h)\psi'_p + (1+g)\psi_w/r_w] - \Omega_w \frac{\partial \psi}{\partial \phi}. \quad (3)$$

In the simulations in this paper, only h or Ω_w are used, and are constant in time. More advanced experimental methods vary the feedback gain in time [30]. The goal here is to demonstrate that feedback or wall rotation can prevent major disruptions, although it can permit minor disruptions.

5 High β NSTX RWTM

RWM and RWTM can be found together at high β . Both can be feedback stabilized. Fig.4 gives an NSTX example [30], with $\beta_N > 4$, above the no wall limit. The feedback

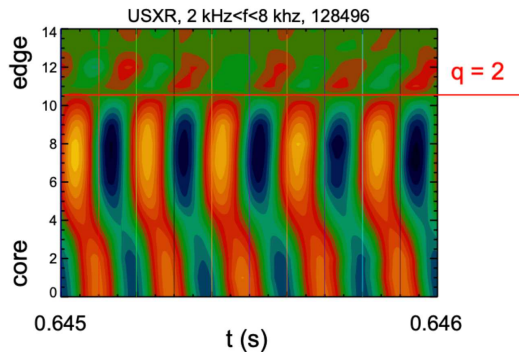


Figure 4: *feedback stabilized (2, 1) RWTM. The RWTM can be identified by its phase inversion at $\rho_{q2} = 0.75$. Reproduced from [30].*

is with complex gain, which can vary in time as the modes grow. Time dependent soft X ray data shows radial mode structure. Initially a locked RWM is stabilized by feedback. It then spins up and converts to a stabilized external kink. It then becomes in Fig.4 a feedback stabilized (2, 1) RWTM. The RWTM can be identified by its phase inversion in soft X ray emission at $\rho_{q2} \approx 0.75$. It is a RWTM because it is close enough to the wall to be affected by the feedback imposed at the wall. This suggests that initially $q_0 > 1$ on axis and $\rho_{q2} < 0.75$. Resistive evolution causes current profile peaking and decreases q_0 on axis, pushing $\rho_{q2} \geq 0.75$. An example is seen in the simulations of Sec.6.

A similar phenomenon is seen was seen in DIII-D [29]. After an ELM, a tearing mode developed in shot 131753 with $\rho_{q2} \approx 0.75$, with growth time $10ms$, when the toroidal velocity at $q_{75} \approx 0$. The mode caused a major disruption, in which the ratio of initial to final β dropped from 1 to less than 0.25.

It appears that RWTMs were observed in KSTAR [31]. A simulation based on an equilibrium reconstruction with $\beta_N = 3.7$ found a (2, 1) mode with magnetic perturbations extending through a resistive wall, clearly a RWTM although not identified as such.

6 High β NSTX simulations

Simulations were done with M3D of modified NSTX equilibrium reconstructions of shot 109070. The simulation parameters were the same as in Sec.3. An example is given in Fig.5 with $\beta_N = 3$. Fig.5(a) gives midplane $q(x)$ profiles, $x = R - R_0$, at nearly

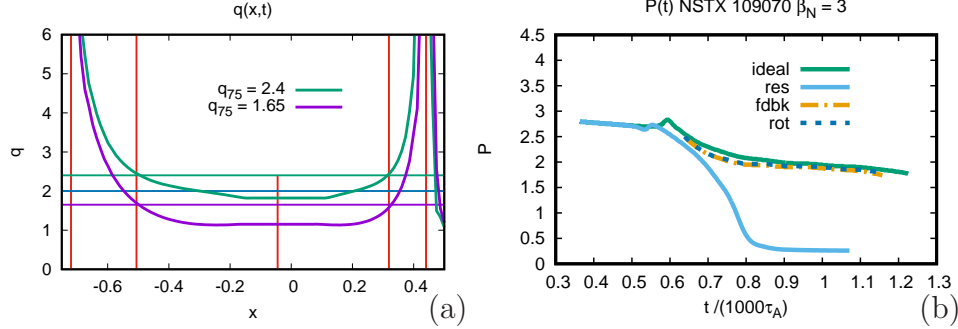


Figure 5: (a) $q(x)$ profiles with evolution to RWTM instability. (b) Time histories of total pressure P with different boundary conditions: ideal wall, resistive wall, feedback, and rotating wall.

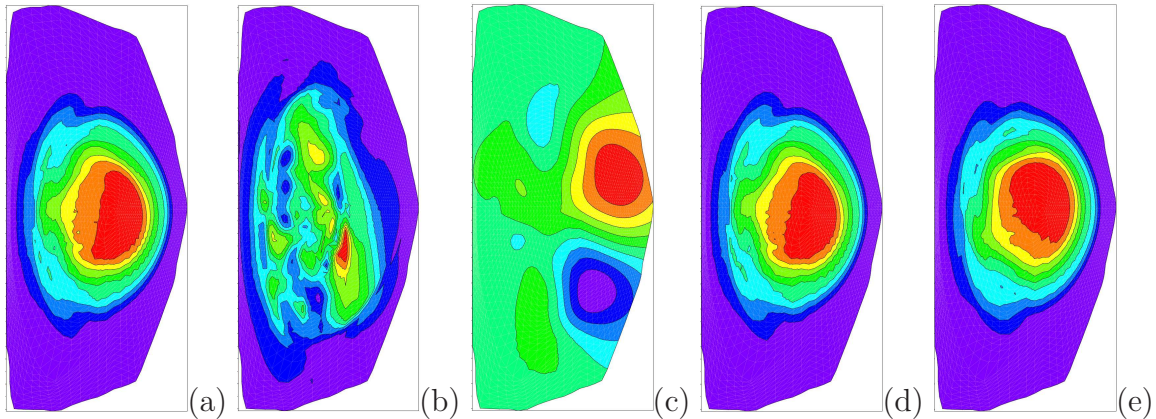


Figure 6: Contours of pressure near the end of the time histories in Fig.5(b). with (a) ideal wall; (b) resistive wall; (c) perturbed magnetic flux of resistive case (b); (d) magnetic feedback; (e) rotating wall.

the initial time, when $q_0 = 1.3$ and $q_{75} = 2.4$. It appears stable to a (2,1) and (3,1) mode. The equilibrium is allowed to evolve resistively, with the current contracting until $q_0 \approx 1$, and $q_{75} = 1.65$. The equilibrium is then RWTM unstable to a (2,1) mode. Fig.5 (b) shows time histories of total pressure P with different boundary conditions: ideal wall, resistive wall, feedback, and wall rotation. Only the case with resistive wall without feedback or wall rotation has a major disruption. The other cases all have minor disruptions. Fig.6 shows contours of pressure with (a) ideal wall; (b) resistive

wall; (d) feedback; (e) rotating wall. A major disruption occurs only with a locked resistive wall. The pressure contours have a large perturbation, as in Fig.3. Fig.6(c) shows $n > 1$ contours of ψ . The perturbations are large lobes which penetrate the wall.

At high β , there are also RWMs, resistive wall external kink modes. Evidently they can also be stabilized by feedback [30] as mentioned in Sec.5. Simulations of RWMs will be presented elsewhere.

7 Dependence of ρ_{q2} on wall position

The critical ρ_{q2} depends on normalized wall radius ρ_w . The critical value $\rho_{q2} = .75$ occurs for $\rho_w = 1.2$, as in DIII-D, NSTX, and the MST model in Sec.3. This can be obtained from a linear model [5] using modified [32] equilibrium profiles with current density $j(\rho) = 0$ for $\rho > \rho_c$, with $j(\rho) = (2/q_0)(1 + \rho^{2\nu})^{-(1+1/\nu)} - c_r$ with $c_r = (1 + \rho_c^{2\nu})^{-(1+1/\nu)}$, and $q(0) = 1$. The profile peakedness parameter ν is determined by ρ_c and q_a . Linear ideal MHD equations for perturbed magnetic flux ψ with mode number (2, 1) were solved in a periodic cylinder. An example is given in Fig.7(a), with $q_a = 2.5$, $\rho_c = 0.7$. The normalized $q = 2$ radius is $\rho_{q2} = 0.9$. Solutions of $\psi(\rho)$ are given for an ideal wall boundary condition $\psi(\rho_w) = 0$ and a no wall boundary condition $d\psi(\rho_w)/d\rho = -2\psi(\rho_w)/\rho_w$. The stability parameter $\Delta' = [\psi'(\rho_{q2+}) - \psi'(\rho_{q2-})]/\psi(\rho_{q2})$ is calculated at ρ_{q2} for ideal and no wall boundary conditions. For an ideal wall, $\Delta' = -0.26$, while for no wall, $\Delta' = 1.38$. This is an unstable RWTM. In Fig.7(b) are plotted curves $\rho_{ci}(\rho_{q2}, \rho_w)$ for $\Delta' = 0$ with ideal wall and $\rho_{cn}(\rho_{q2})$ with $\Delta' = 0$ for no wall. Three ρ_{ci} curves are plotted, for $\rho_w = 1.1, 1.2, 1.5$. There is only one $\rho_{cn}(\rho_{q2})$ curve, since it does not depend on ρ_{wall} . The RWTM is unstable for $\rho_{ci} \geq \rho_c \geq \rho_{cn}$. The onset condition for RWTM is $\rho_{ci} = \rho_{cn}$. For $\rho_w = 1.2$, $\rho_{q2} = 0.75$ as in Fig.1(b).

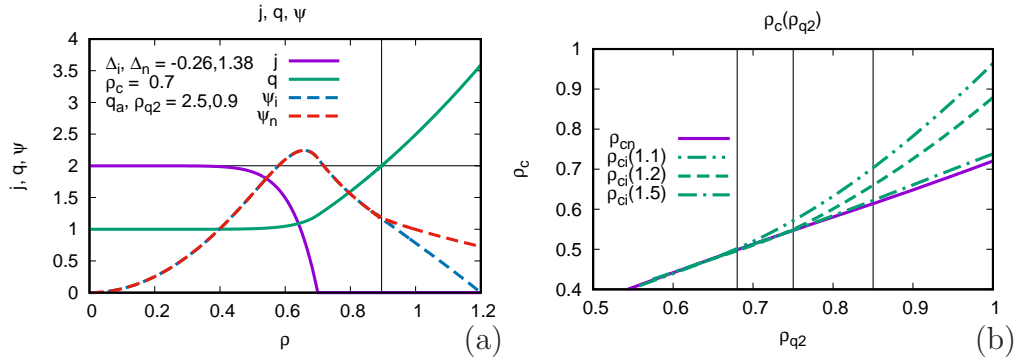


Figure 7: (a) ψ , j , and q , with ψ for ideal (ψ_1) and no wall (ψ_2). (b) Curves of $\rho_{ci}(\rho_{q2})$, $\rho_{cn}(\rho_{q2})$ and $q_a(\rho_{q2})$ for $\rho_w = 1.1, 1.2, 1.5$.

Fig.7(b) gives a relation between ρ_{q2} and ρ_w , shown in Fig.8(a). The value of ρ_{q2}/ρ_w as a function of ρ_{q2} is approximately constant. The data in Fig.8(a) can be fit as follows.

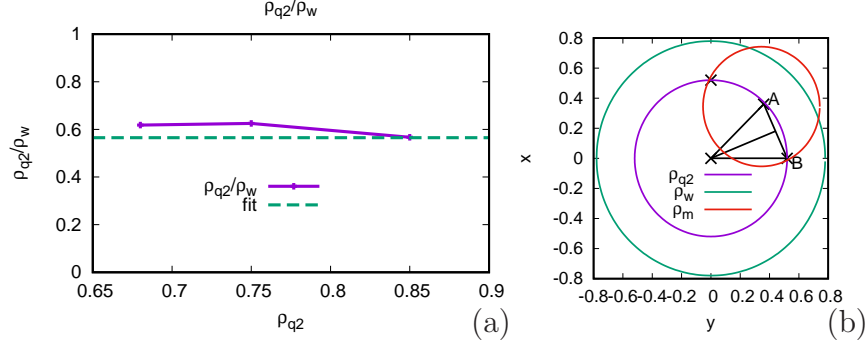


Figure 8: (a) ρ_{q2}/ρ_w depends weakly on ρ_{q2} . (b) model of wall interaction of $(m, n) = (2, 1)$ mode.

The magnetic $n \geq 1$ perturbations shown in Fig.3(c) and Fig.6(c) are lobes which extend into the wall. In Fig.8(b), an (m, n) mode is modeled as dividing the contour $\rho = \rho_{q2}$ into $2m$ arcs with ends at angles $0, \pi/m, \dots$. A chord of length $2 \sin(\pi/2m)\rho_{q2}$ can be drawn connecting the midpoint of the arc labelled ‘‘A’’ to the intersection of the arc with the x axis at ‘‘B’’. This is the radius ρ_m of a circle drawn through the midpoint of the arc ‘‘A’’, as shown in Fig.8(b). It models a lobe of a (m, n) mode structure. The radius of the circle must be large enough to intersect the wall, such that $\rho_w \leq \rho_{q2} + \rho_m$. This can be expressed

$$\frac{\rho_w}{\rho_{q2}} \leq 1 + 2 \sin\left(\frac{\pi}{4m}\right) \quad (4)$$

which is $\rho_w/\rho_{q2} = 1.77$ for $m = 2$, $\rho_w/\rho_{q2} = 1.52$ for $m = 3$. This is shown as the fit in Fig.8(a). The calculated line in Fig.8(a) intersects the fit at $\rho_{q2} = 0.85$, where according to Fig.7(b), $\rho_w = 1.5$. This suggests that for larger ρ_w , the wall is too far away to interact with the mode.

8 Summary

To summarize, resistive wall tearing modes (RWTM) can cause major disruptions. A signature of RWTMs is that the rational surface is sufficiently close to the wall. For $(m, n) = (2, 1)$ modes, the rational surface radius of the $q = 2$ surface, normalized to the plasma minor radius, is $\rho_{q2} > 0.75$. This can also be expressed as the value of q at $\rho = 0.75$, $q_{75} < 2$. The domain of instability of RWTMs in the (q_{75}, β) plane was presented qualitatively. The $\rho_{q2} > 0.75$ criterion was found in a DIII-D locked mode disruption database. The importance of mode locking and disruption precursors was discussed.

A very important feature of RWTMs is that they produce major disruptions when the $q_{75} < 2$ criterion is satisfied. If this is not satisfied, or if the wall is ideally conduct-

ing, then the mode becomes a tearing mode and does not produce a major disruption, although it can produce a minor disruption. Feedback, or rotation of the mode at the wall by complex feedback, can emulate an ideal wall. This was verified in simulations of a sequence of low β equilibria. It was shown that when the wall is resistive and the q_{75} criterion is satisfied, the saturated mode amplitude is large, otherwise it is small. The computational model used for feedback and rotating wall was discussed.

At high β , feedback stabilized $(2, 1)$ modes were observed in NSTX with $\rho_{q2} \approx 0.75$, indicating wall interaction, implying a RWTM. In DIII-D, modes with $\rho_{q2} \approx 0.75$ caused a major disruption. Simulations were performed using modified NSTX equilibria at moderate $\beta_N = 3$, which satisfied $q_{75} < 2$, and produced major disruptions with a resistive wall, minor disruptions with an ideal wall, feedback, or rotating wall.

The q_{75} criterion was analyzed in a linear simulations, and a simple geometric model was given. The criterion depends weakly on the ratio of ρ_{q2}/ρ_w , where ρ_w is the wall radius normalized to plasma radius. For $\rho_w > 1.5$, the wall is too far away for a RWTM and feedback stabilization is not possible. The criterion is also obtained for general (m, n) , and requires the rational surface to be closer to the wall.

In conclusion, $(m, n) = (2, 1)$ RWTMs satisfy the $q_{55} < 2$ condition. The boundary conditions at the wall can prevent a major disruption. With an ideally conducting wall, tearing modes produce only minor disruptions. Feedback and rotating wall boundary conditions act like an ideal wall. This could potentially eliminate disruptions from tokamaks, greatly enhancing the prospects of magnetic fusion.

Acknowledgement Thanks to S. Sabbagh for pointing out the possible RWTM in [30]. This work was supported by U.S. D.O.E. grant DE-SC0020127.

References

- [1] H. Strauss and JET Contributors, Effect of Resistive Wall on Thermal Quench in JET Disruptions, *Phys. Plasmas* **28**, 032501 (2021)
- [2] H. Strauss, Thermal quench in ITER disruptions, *Phys. Plasmas* **28** 072507 (2021)
- [3] H. Strauss, B. C. Lyons, M. Knolker, Locked mode disruptions in DIII-D and application to ITER, *Phys. Plasmas* **29** 112508 (2022);
- [4] H. R. Strauss, B. E. Chapman, N. C. Hurst, MST Resistive Wall Tearing Mode Simulations, *Plasma Phys. Control. Fusion* **65** 084002 (2023).
- [5] H. R. Strauss, Models of resistive wall tearing mode disruptions, *Phys. Plasmas* **30**, 112507 (2023); doi:10.1063/5.0172375
- [6] H. R. Strauss, B. E. Chapman, B. C. Lyons, Resistive Wall Tearing Mode Disruptions, *Nucl. Fusion* **64** 106037 (2024); doi:10.1088/1741-4326/ad7272

- [7] R. Sweeney, W. Choi, M. Austin, M. Brookman, V. Izzo, M. Knolker, R.J. La Haye, A. Leonard, E. Strait, F.A. Volpe and The DIII-D Team, Relationship between locked modes and thermal quenches in DIII-D, *Nucl. Fusion* **58**, 056022 (2018)
- [8] R. Sweeney, W. Choi, R. J. La Haye, S. Mao, K. E. J. Olofsson, F. A. Volpe, and the DIII-D Team, Statistical analysis of $m/n = 2/1$ locked and quasi - stationary modes with rotating precursors in DIII-D, *Nucl. Fusion* **57** 0160192 (2017).
- [9] F. Troyon, A.Roy, W.A.Cooper, F.Yasseen, A.Tumbull, Beta limit in tokamaks: experimental and computational status, *Plasma Physics and Controlled Fusion* textbf30, 1597 (1988).
- [10] R. Betti, Beta limits for the $n = 1$ mode in rotating - toroidal - resistive plasmas surrounded by a resistive wall, *Phys. Plasmas* **5**, 3615 (1998).
- [11] H. R. Strauss, Linjin Zheng, M. Kotschenreuther, W.Park, S. Jardin, J. Breslau, A.Pletzer, R. Paccagnella, L. Sugiyama, M. Chu, M. Chance, A. Turnbull, Halo Current and Resistive Wall Simulations of ITER, paper TH/2 - 2, 20th IAEA Fusion Energy Conference 2004, Villamora, Portugal (2004).
- [12] S.N. Gerasimov, P. Abreu, G. Artaserse, M. Baruzzo, P. Buratti, I.S. Carvalho, I.H. Coffey, E. De La Luna, T.C. Hender, R.B. Henriques, R. Felton, S. Jachmich, U. Kruezi, P.J. Lomas, P. McCullen, M. Maslov, E. Matveeva, S. Moradi, L. Piron1, F.G. Rimini, W. Schippers, C. Stuart, G. Szepesi, M. Tsalas, D. Valcarcel, L.E. Zakharov and JET Contributors, Overview of disruptions with JET-ILW, *Nucl. Fusion* **60** 066028 (2020).
- [13] S. Wang, Z. W. Ma, Influence of toroidal rotation on resistive tearing modes in tokamaks, *Phys. Plasmas* **22**, 122504 (2015); doi:10.1063/1.4936977
- [14] R. Coelho, E. Lazzaro, Effect of sheared equilibrium plasma rotation on the classical tearing mode in a cylindrical geometry, *Phys. Plasmas* **14**, 012101 (2007)
- [15] H. R. Strauss, Rotational stabilization of drift tearing modes, *Phys. Fluids* **B 4** 3 (1992); doi:10.1063/1.860448
- [16] J. A. Finn, Resistive wall stabilization of kink and tearing modes, *Phys. Plasmas* **2**, 198 (1995)
- [17] F.C. Schuller, Disruptions in tokamaks, *Plasma Phys. Controlled Fusion* **37**, A135 (1995).
- [18] J.A. Wesson, R.D. Gill, M. Hugon, F.C. Schuller, J.A. Snipes, D.J. Ward, D.V. Bartlett, D.J. Campbell, P.A. Duperrex, A.W. Edwards, R.S. Granetz, N.A.O. Gottardi, T.C. Hender, E. Lazzaro, P.J. Lomas, N. Lopes Cardozo, K. F. Mast, M.F.F. Nave, N.A. Salmon, P. Smeulders, P.R. Thomas, B.J.D. Tubbing, M.F. Turner, A. Weller, Disruptions in JET, *Nucl. Fusion* **29** 641 (1989).

- [19] M. Giacomini, A. Pau, P. Ricci, O. Sauter, T. Eich, the ASDEX Upgrade team, JET Contributors, and the TCV team, First-Principles Density Limit Scaling in Tokamaks Based on Edge Turbulent Transport and Implications for ITER Phys. Rev. Lett. **128**, 185003 (2022)
- [20] G. Pucella, P. Buratti, E. Giovannozzi, E. Alessi, F. Auremma, D. Brunetti, D. R. Ferreira, M. Baruzzo, D. Frigione, L. Garzotti, E. Joffrin, E. Lerche, P. J. Lomas, S. Nowak, L. Piron, F. Rimini, C. Sozzi, D. Van Eester, and JET Contributors, Tearing modes in plasma termination on JET: the role of temperature hollowing and edge cooling, Nucl. Fusion **61** 046020 (2021)
- [21] D. A. Gates, D. P. Brennan, L. Delgado-Aparicio, and R. B. White, The tokamak density limit: A thermo-resistive disruption mechanism, Phys. Plasmas **22**, 060701 (2015); <https://doi.org/10.1063/1.4922472>
- [22] V. A. Izzo, D. G. Whyte, R. S. Granetz, P. B. Parks, E. M. Hollmann, L. L. Lao, J. C. Wesley, Magnetohydrodynamic simulations of massive gas injection into Alcator C - Mod and DIII-D plasmas, Phys. Plasmas **15**, 056109 (2008).
- [23] M. Okabayashi, P. Zanca, E.J. Strait, A.M. Garofalo, J.M. Hanson, Y. In5, R.J. La Haye, L. Marrelli, P. Martin, R. Paccagnella, C. Paz-Soldan, P. Piovesan, C. Piron, L. Piron, D. Shiraki, F.A. Volpe and The DIII-D and RFX-mod Teams, Avoidance of tearing mode locking with electro-magnetic torque introduced by feedback-based mode rotation control in DIII-D and RFX-mod, Nuclear Fusion **57**, 016035 (2017)
- [24] W. Park, E. Belova, G. Y. Fu, X. Tang, H. R. Strauss, L. E. Sugiyama, Plasma Simulation Studies using Multilevel Physics Models, Phys. Plasmas **6**, 1796 (1999).
- [25] A. Bondeson, Yueqiang Liu, D. Gregoratto, Y. Gribov and V.D. Pustovitov, Active control of resistive wall modes in the large-aspect-ratio tokamak, Nucl. Fusion **42** (2002) 768–779
- [26] Yuling He, Yueqiang Liu, Xu Yang, Guoliang Xia, Li Li, Active control of resistive wall mode via modification of external tearing index, Physics of Plasmas **28**, 012504 (2021)
- [27] D. P. Brennan, J. M. Finn, Control of linear modes in cylindrical resistive magnetohydrodynamics with a resistive wall, plasma rotation, and complex gain, Phys. Plasmas **21**, 102507 (2014).
- [28] A.M. Garofalo, G.L. Jackson, R.J. La Haye, M. Okabayashi, H. Reimerdes, E.J. Strait, J.R. Ferron, R.J. Groebner, Y. In, M.J. Lanctot, G. Matsunaga, G.A. Navratil, W.M. Solomon, H. Takahashi, M. Takechi, A.D. Turnbull and the DIII-D Team, Stability and control of resistive wall modes in high beta, low rotation DIII-D plasmas, Nucl. Fusion **47** 1121–1130 (2007).

- [29] M. Okabayashi, I.N. Bogatu, M.S. Chance, M.S. Chu, A.M. Garofalo, Y. In, G.L. Jackson, R.J. La Haye, M.J. Lanctot, J. Manickam, L. Marrelli, P. Martin, G.A. Navratil, H. Reimerdes, E.J. Strait, H. Takahashi, A.S. Welander, T. Bolzonella, R.V. Budny, J.S. Kim, R. Hatcher, Y.Q. Liu and T.C. Luce, Comprehensive control of resistive wall modes in DIII-D advanced tokamak plasmas, *Nucl. Fusion* 49 (2009) 125003.
- [30] S. A. Sabbagh, S.P. Gerhardt, J.E. Menard, R. Betti, D.A. Gates, B. Hu, O.N. Katsuro-Hopkins, B.P. LeBlanc, F.M. Levinton, J. Manickam, K. Tritz and H. Yuh, Advances in global MHD mode stabilization research on NSTX, *Nucl. Fusion* 50 025020 (2010).
- [31] Y.S. Park, S.A. Sabbagh, J.H. Ahn, B.H. Park, H.S. Kim, J.W. Berkery, J.M. Bialek, Y. Jiang, J.G. Bak, A.H. Glasser, J.S. Kang, J. Lee, H.S. Han, S.H. Hahn, Y.M. Jeon, J.G. Kwak, H.K. Park, Z.R. Wang, J.-K. Park, N.M. Ferraro and S.W. Yoon, Analysis of MHD stability and active mode control on KSTAR for high confinement, disruption-free plasma, *Nucl. Fusion* 60 056007 (2020); doi:10.1088/1741-4326/ab79ca
- [32] H. P. Furth, P. H. Rutherford, and H. Selberg, Tearing mode in the cylindrical tokamak, *Physics of Fluids* 16, 1054 (1973)